BMJ Open Respiratory Research

Knockdown of KIF23 alleviates the progression of asthma by inhibiting pyroptosis

Xingyu Rao,[1] Zicheng Lei,[1] Huifang Zhu,[1] Kaiyuan Luo,[1] Chaohua Hu [2]

To cite: Rao X, Lei Z, Zhu H, *et al*. Knockdown of KIF23 alleviates the progression of asthma by inhibiting pyroptosis. *BMJ Open Respir Res* 2024;**11**:e002089. doi:10.1136/bmjresp-2023-002089

► Additional supplemental material is published online only. To view, please visit the journal online (https://doi.org/10.1136/bmjresp-2023-002089).

Received 25 September 2023
Accepted 14 March 2024

[1]Department of Pediatrics, First Affiliated Hospital of Gannan Medical University, Ganzhou, Jiangxi, China
[2]Department of Surgery I, Third Affiliated Hospital of Gannan Medical University, Ganzhou, Jiangxi, China

Correspondence to
Dr Chaohua Hu;
huchaohua0210@126.com

ABSTRACT

Background Asthma is a chronic disease affecting the lower respiratory tract, which can lead to death in severe cases. The cause of asthma is not fully known, so exploring its potential mechanism is necessary for the targeted therapy of asthma.

Method Asthma mouse model was established with ovalbumin (OVA). H&E staining, immunohistochemistry and ELISA were used to detect the inflammatory response in asthma. Transcriptome sequencing was performed to screen differentially expressed genes (DEGs). The role of KIF23 silencing in cell viability, proliferation and apoptosis was explored by cell counting kit-8, EdU assay and flow cytometry. Effects of KIF23 knockdown on inflammation, oxidative stress and pyroptosis were detected by ELISA and western blot. After screening KIF23-related signalling pathways, the effect of KIF23 on p53 signalling pathway was explored by western blot.

Results In the asthma model, the levels of caspase-3, IgG in serum and inflammatory factors (interleukin (IL)-1β, KC and tumour necrosis factor (TNF)-α) in serum and bronchoalveolar lavage fluid were increased. Transcriptome sequencing showed that there were 352 DEGs in the asthma model, and 7 hub genes including *KIF23* were identified. Knockdown of KIF23 increased cell proliferation and inhibited apoptosis, inflammation and pyroptosis of BEAS-2B cells induced by IL-13 in vitro. In vivo experiments verified that knockdown of *KIF23* inhibited oxidative stress, inflammation and pyroptosis to alleviate OVA-induced asthma mice. In addition, p53 signalling pathway was suppressed by KIF23 knockdown.

Conclusion Knockdown of KIF23 alleviated the progression of asthma by suppressing pyroptosis and inhibited p53 signalling pathway.

WHAT IS ALREADY KNOWN ON THIS TOPIC

⇒ Pyroptosis plays an important role in asthma, and the role of KIF23 in asthma is unknown.

WHAT THIS STUDY ADDS

⇒ Knockdown of KIF23 alleviates asthma by inhibiting pyroptosis.

HOW THIS STUDY MIGHT AFFECT RESEARCH, PRACTICE OR POLICY

⇒ This study provides a new target in the therapy of asthma.

INTRODUCTION

Asthma is a chronic disease affecting the lower respiratory tract.[1 2] The main manifestations are airway swelling and inflammation, and bronchospasm, which can lead to dyspnoea.[2] Clinically, patients with asthma show recurrent wheezing, chest tightness, cough and shortness of breath,[1] which can lead to death in severe cases.[3] The cause of asthma is not yet known, but asthma can be triggered by many risk factors. Genetic factors greatly increase the risk of asthma.[4] Common causes of asthma include respiratory virus infection, particulate matter (PM) pollution, allergens and stress.[5] Taking medications and avoiding things that trigger asthma are common means of controlling asthma. Therefore, exploring its potential mechanism is necessary for the targeted therapy of asthma.

Kinesin family member 23 (KIF23), also known as MKLP-1, is involved in mitosis and meiosis,[6 7] and is crucial in the development of human cancers.[8] Evidence has shown that KIF23 interacts with Amer1 to activate the Wnt/β-catenin signalling pathway, contributing to gastric cancer development.[9] Jin *et al* find that elevated KIF23 can activate the Wnt/β-catenin pathway, thereby promoting colorectal cancer progression.[10] In addition, high expression of KIF23 is associated with poor prognosis of pancreatic ductal adenocarcinoma, and knockdown of KIF23 inhibits proliferation, which may be a potential target for the treatment of pancreatic ductal adenocarcinoma.[11] Inhibition of KIF23 alleviates idiopathic pulmonary arterial hypertension by inhibiting pyroptosis, and KIF23 may regulate pyroptosis through PI3K/AKT and MAPK pathways.[12] However, the mechanism of KIF23-regulating asthma is not clear.

Pyroptosis is a type of programmed cell death mediated by inflammasomes, which is activated by caspases and cleaved GSDMD, usually accompanied by the release of

inflammatory factors.[13] Researchers have found that pyroptosis is widespread in various respiratory diseases. Excessive pyroptosis may cause airway inflammation and tissue damage, triggering an inflammatory response that leads to more severe damage and poor prognosis in respiratory diseases.[14] Caspase-11-mediated pyroptosis promotes the progression of endotoxaemia-induced lung injury, which is an important therapeutic target for acute lung injury.[15] Inhibition of pyroptosis alleviates lung inflammation and fibrosis progression induced by silica.[16] Zhuang *et al* have found that NLRP3-activated bronchial epithelial pyroptosis aggravates airway inflammation in asthma.[17] However, the role of KIF23 in pyroptosis is uncharted in asthma.

In our study, transcriptome sequencing was carried out to screen the differentially expressed genes (DEGs) on the mouse model of asthma. Afterwards, we explored the role of KIF23 in asthma and its influence on cell proliferation, apoptosis, inflammation, oxidative stress and pyroptosis through in vitro and in vivo experiments. Subsequently, p53 pathway was significantly enriched in asthma by screening genes and the role of KIF23 in this pathway was explored, which will provide a new target in the therapy of asthma.

MATERIALS AND METHODS

Construction of asthma mouse model

BALB/c mice (6–7 weeks, 18–20 g) were obtained from SPF Biotechnology Co (Beijing, China) and randomly grouped into control and OVA (ovalbumin) (n=6). In OVA group, mice were injected intraperitoneally with 50 µL aluminium hydroxide, 5 µL 1% OVA and 70 µL phosphate-buffered saline (PBS) on the first day of the experiment to conduct an asthma model. On the 7th–14th day, mice were nebulised with 1% OVA (0.1 g OVA, 10 mL PBS) for about 1 hour.

Another 24 BALB/c mice (6–7 weeks, 18–20 g, SPF) were randomly divided into normal, control, lv-sh-NC (injected with lentivirus encoding negative control shRNA) and lv-sh-KIF23 (injected with lentivirus encoding *Kif23* shRNA) on average. The lentiviral particles encoding *Kif23* shRNA or negative control shRNA (5.0×10^7 IU, 100 µL) were subcutaneously injected into the shaved dorsal skin of the mice on the seventh day before OVA nebulisation. Except the normal group, mice in other three groups received 1% OVA to conduct the asthma model. After the last day of atomisation, all mice were anaesthetised by isoflurane inhalation and sacrificed by cervical dislocation. Subsequently, mice were intubated by tracheotomy, and part of the lung lobes was perfused with pre-cooled PBS (0.5 mL) for three consecutive times.[18] Bronchoalveolar lavage fluid (BALF) was collected and stored at −80°C for subsequent experiments. In addition, serum and lung tissues were obtained for following experiments. Partial lung tissues were taken after perfusion for staining observation.

Patient and public involvement

None.

H&E staining

The lung tissue was fixed in paraformaldehyde solution (4%). The next day, the tissue was washed and dehydrated gradiently with ethanol. Afterwards, the tissue was embedded in paraffin. Paraffin slices were then stained with H&E. Finally, the slices were dehydrated and sealed with neutral balsam.

Immunohistochemistry

Paraffin-embedded sections were dewaxed and rehydrated, and 10 mmol/L EDTA was used for antigen repair. At room temperature, slices were incubated with 0.3% H_2O_2 to inactivate endogenous peroxidase. After that, the samples were blocked with 3% bovine serum albumin and incubated with anti-caspase-3 (ab184787, 1:1000, Abcam, Cambridge, USA) overnight at 4°C. Subsequently, the samples were incubated with goat anti-rabbit secondary antibody (Abcam) at 37°C for 1 hour. Then 5% DAB staining solution was used for developing. After H&E staining, the sections were decolourised, dehydrated and sealed.

Enzyme-linked immunosorbent assay

The levels of IgG, mouse CXCL1/KC, interleukin (IL)-18, IL-1β and tumour necrosis factor (TNF)-α were evaluated by corresponding ELISA kits (Esebio, Shanghai, China). Cell supernatant, serum and BALF samples in each group were added into each well and reacted with horseradish peroxidase (HRP)-labelled detection antibody, and then the plate was incubated for 60 min at 37°C. The liquid was removed, and the plate was washed. Substrates A and B were added, and the plate was incubated in the dark at 37°C for 15 min. Total 50 µL of stopping solution was added to each well, and the optical density (OD) value was measured at 450 nm within 15 min.

Transcriptome sequencing

Three lung tissue samples were taken from control and model group for RNA sequencing (RNA-seq). TRIzol was applied to extract total RNA from each sample. Total 2 µg of RNA per sample was taken to conduct the sequencing libraries. Transcriptome sequencing was performed on Illumina Novaseq 6000 sequencing platform, and paired-end clean reads were aligned to mm10 using HISAT2 V.2.0.5. Differential analysis of gene expression was performed using DESeq, and the screening condition of DEGs was set as $|\log_2\text{FoldChange}|>1$, $p<0.05$. The volcano map of DEGs was plotted using the R language ggplots2. Biocluster analysis of common DEGs was performed using the R language Pheatmap package.

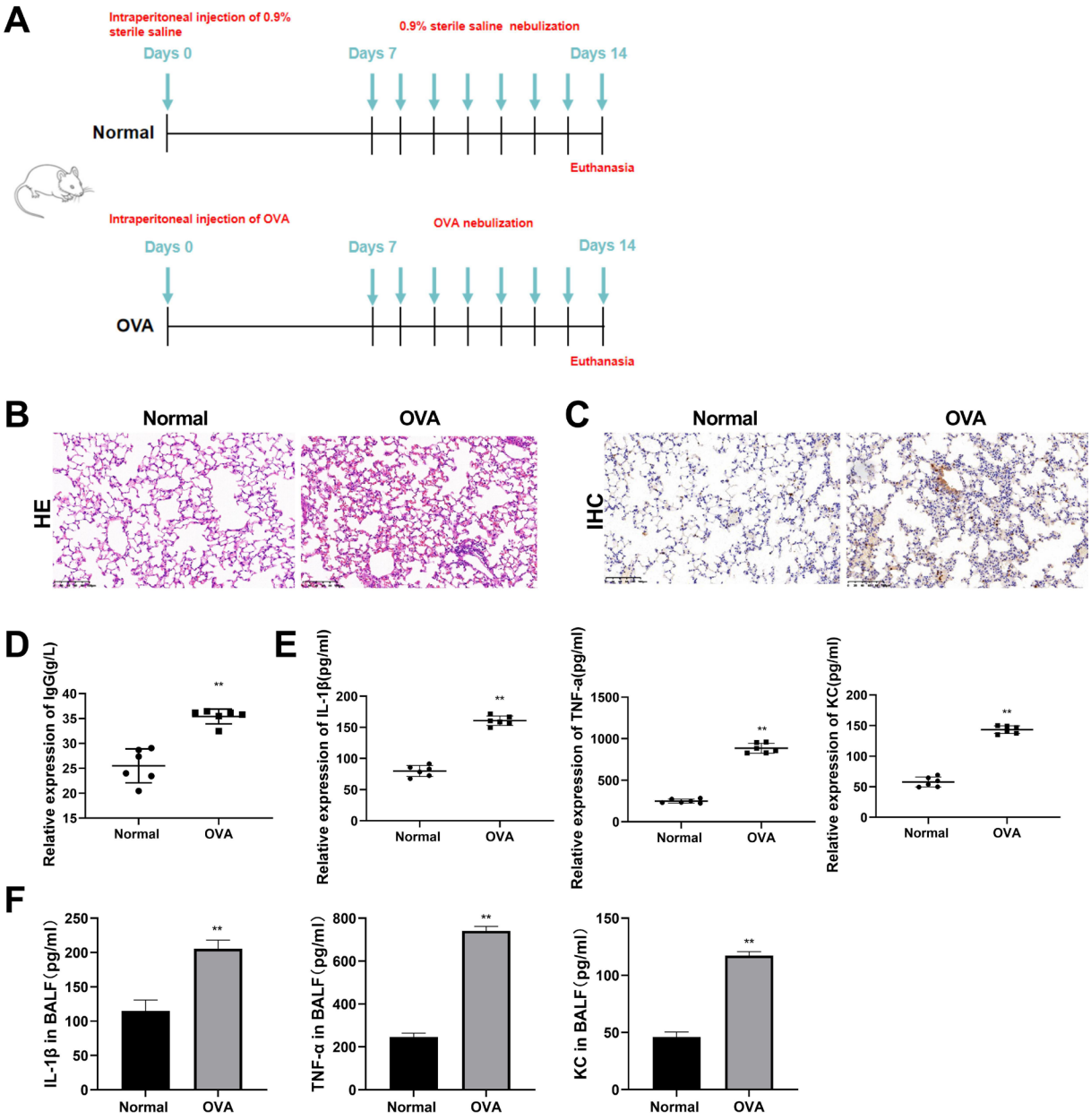

Figure 1 Construction of asthma mouse model. (A) Experimental protocol of asthma mouse model induced by OVA. (B) H&E staining (magnification: 200×, scale bar: 100 µm). (C) Immunohistochemistry (IHC) was used to detect caspase-3 (magnification: 200×, scale bar: 100 µm). (D) ELISA was performed to detect the level of IgG epitopes in the serum of mice. (E) ELISA was performed to detect the expression level of inflammatory factors (KC, IL-1β and TNF-α) in serum of mice. (F) ELISA was used to detect the levels of inflammatory factors (KC, IL-1β and TNF-α) in bronchoalveolar lavage fluid (BALF) of mice. **P<0.01 vs normal (n=6). IL, interleukin; OVA, ovalbumin; TNF, tumour necrosis factor.

Functional analysis of DEGs

Gene Ontology (GO) and Kyoto Encyclopedia of Genes and Genomes (KEGG) analyses were performed on DEGs by DAVID (https://david.ncifcrf.gov/summary.jsp). Significance was set at $p<0.05$. The degree of enrichment was measured by Rich factor, false discovery rate value and the number of genes enriched to GO term or KEGG pathway. Bubble plots of GO and KEGG enrichment were generated.

Analysis of hub genes

The DEGs and pyroptosis-related genes were plotted by Venn diagram. The intersected common genes were analysed by Cytoscape. The top six genes with the highest score were selected and displayed.

Screen of signalling pathways

Genecard and Coxpresdb databases were performed to screen the genes co-expressed with *Kif23* in asthma. KEGG enrichment of co-expressed genes was

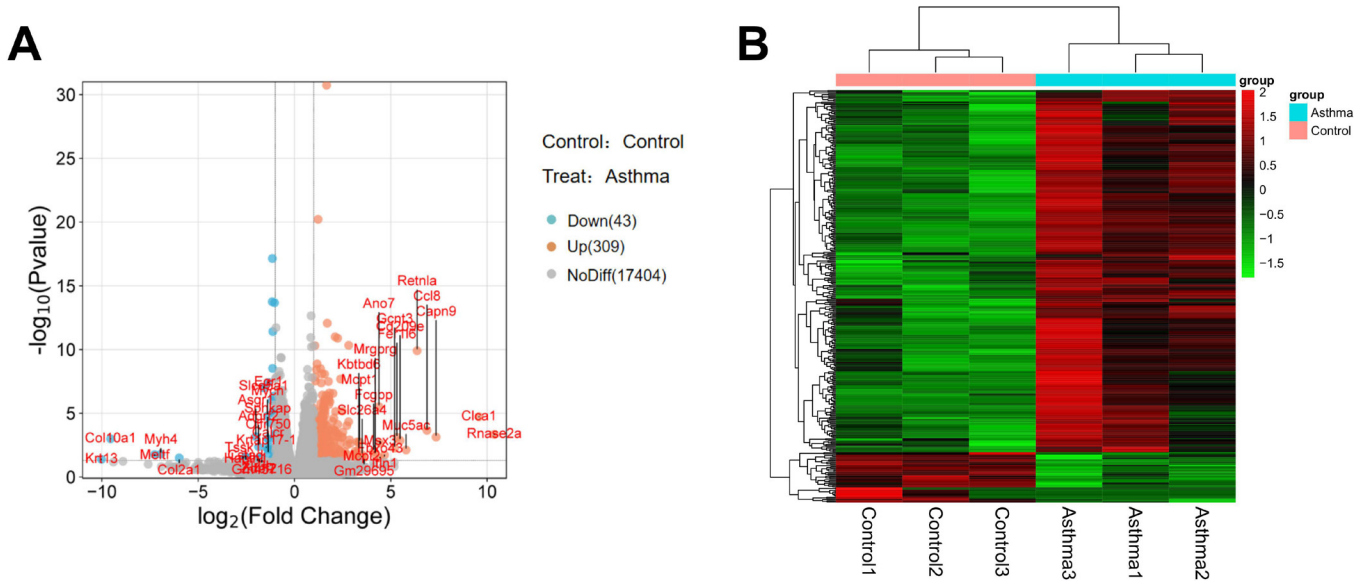

Figure 2 Analysis of differentially expressed genes (DEGs). (A) Volcano plot of DEGs. Top 20 upregulated and downregulated DEGs were marked. (B) Cluster analysis of DEGs.

analysed by DAVID and bubble plot of KEGG enrichment was drawn.

Real-time fluorescence quantitative PCR

TRIzol reagent (Invitrogen, USA) was used to extract total RNA. The concentration of RNA was measured by ultraviolet spectrophotometer. The ratio of OD260/OD280 was between 1.9 and 2.0, indicating that the purity was high. The cDNA template was synthesised by PCR amplification, and real-time fluorescence quantitative PCR (RT-qPCR) was performed using the ABI7500 quantitative PCR instrument (Applied Biosystems, USA). The reaction conditions were: 95°C pre-denaturation for 30 s, 95°C denaturation for 10 s, 60°C annealing for 30 s, 40 cycles. *Gapdh* was chosen as internal control. The obtained cycle threshold value was analysed by $2^{-\Delta\Delta Ct}$ method. Primer sequences were shown in online supplemental table 1.

Western blotting

Cells were treated with radioimmunoprecipitation assay lysis buffer to isolate total proteins. Protein concentration was inspected by Pierce BCA Protein Assay Kit (Thermo Fisher Scientific, Waltham, Massachusetts, USA). Proteins were separated by 10% sodium dodecyl sulphate-polyacrylamide gel electrophoresis (SDS-PAGE) and then transferred to a polyvinylidene difluoride membrane. The membrane was sealed in 5% skim milk, and then incubated with

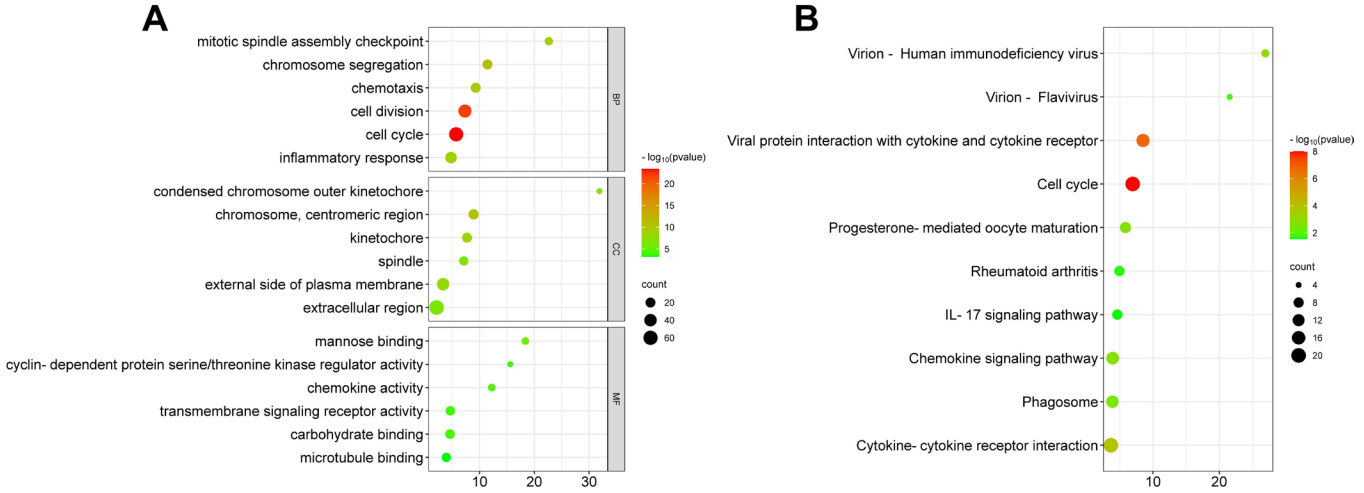

Figure 3 GO and KEGG enrichment analysis of DEGs. (A) Bubble plot of GO enrichment analysis. (B) Bubble plot of KEGG enrichment analysis. DEGs, differentially expressed genes; GO, Gene Ontology; IL, interleukin; KEGG, Kyoto Encyclopedia of Genes and Genomes.

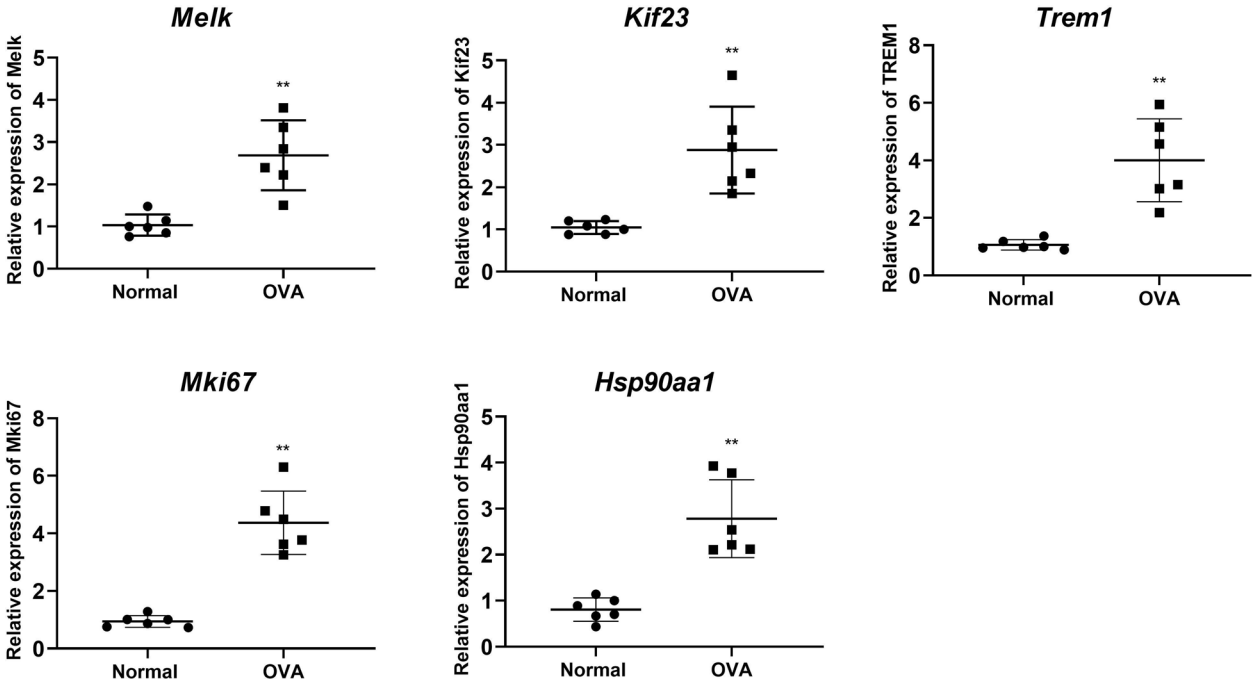

Figure 4 Real-time fluorescence quantitative PCR detection of hub genes in lung tissues. **P<0.01 vs normal (n=6). OVA, ovalbumin.

primary antibodies, including anti-KIF23 (ab174304, 1:1000, Abcam), anti-GSDMD (ab219800, 1:1000, Abcam), anti-NLRP3 (ab263899, 1:1000, Abcam), anti-ASC (ab283684, 1:1000, Abcam), anti-p53 (ab32389, 1:1000, Abcam), anti-p21 (ab188224, 1:1000, Abcam), anti-BAX (ab32503, 1:1000, Abcam) and anti-GAPDH (ab9485, 1:2000, Abcam), overnight at 4°C. Afterwards, it was incubated with goat anti-rabbit secondary antibody (Abcam) for 1 hour at room temperature. Finally, enhanced chemiluminescence solution was added for developing, and images were captured on Tanon 5200 Chemiluminescent Imaging System.

Cell culture and transfection

BEAS-2B cells (h023, iCell, Shanghai, China) were cultured in RPMI-1640 medium (Hyclone, USA) containing 10% fetal bovine serum (Gibco, USA) at 37°C, 5% CO_2. Cells were divided into four groups: normal; control; si-NC (cells were transfected with negative control siRNA); si-KIF23 (cells were transfected with KIF23 siRNA-1/2/3). siRNAs were synthesised from Ribobio (Guangzhou, China). Except the normal group, the other three groups of cells were treated with IL-13 (10 ng/mL) for 24 hours to construct asthma cell model.

Cell counting kit-8 assay

Cell counting kit-8 (CCK-8) assay was used to detect cell viability. BEAS-2B cells (1×10^4 cells/well) were incubated in 96-well plates. After incubation for 24 hours, 10 µL of CCK-8 (Beyotime, Shanghai, China) was added, and then the cells were incubated for 2 hours in the dark. Finally, the absorbance at 450 nm was determined by a microplate reader.

EdU assay

BEAS-2B cells were incubated in 96-well plates. The experiment was performed following the instructions of EdU kit (Beyotime). Subsequently, the nucleus was restained with Hoechst 33, 342 (Beyotime). Results were observed and then photographed under a fluorescence microscope, and EdU positive cells were calculated.

Flow cytometry

BEAS-2B cells were collected and washed with PBS. Cells were suspended with 300 µL of 1×binding buffer. Subsequently, 5 µL of Annexin V-FITC was added and cells were incubated in the dark at room temperature for 15 min. Then, 5 µL of propidium iodide (PI) solution was added to the cell suspension for fluorescence labelling. Apoptosis of cells was detected by a flow cytometry.

Statistical analysis

All statistical analyses were performed using GraphPad Prism V.8.0 software. Data were expressed as mean±SD. t-test was used for comparisons between two groups, and one-way analysis of variance (ANOVA) was used for comparisons between multiple groups. Tukey's multiple comparisons test was used for

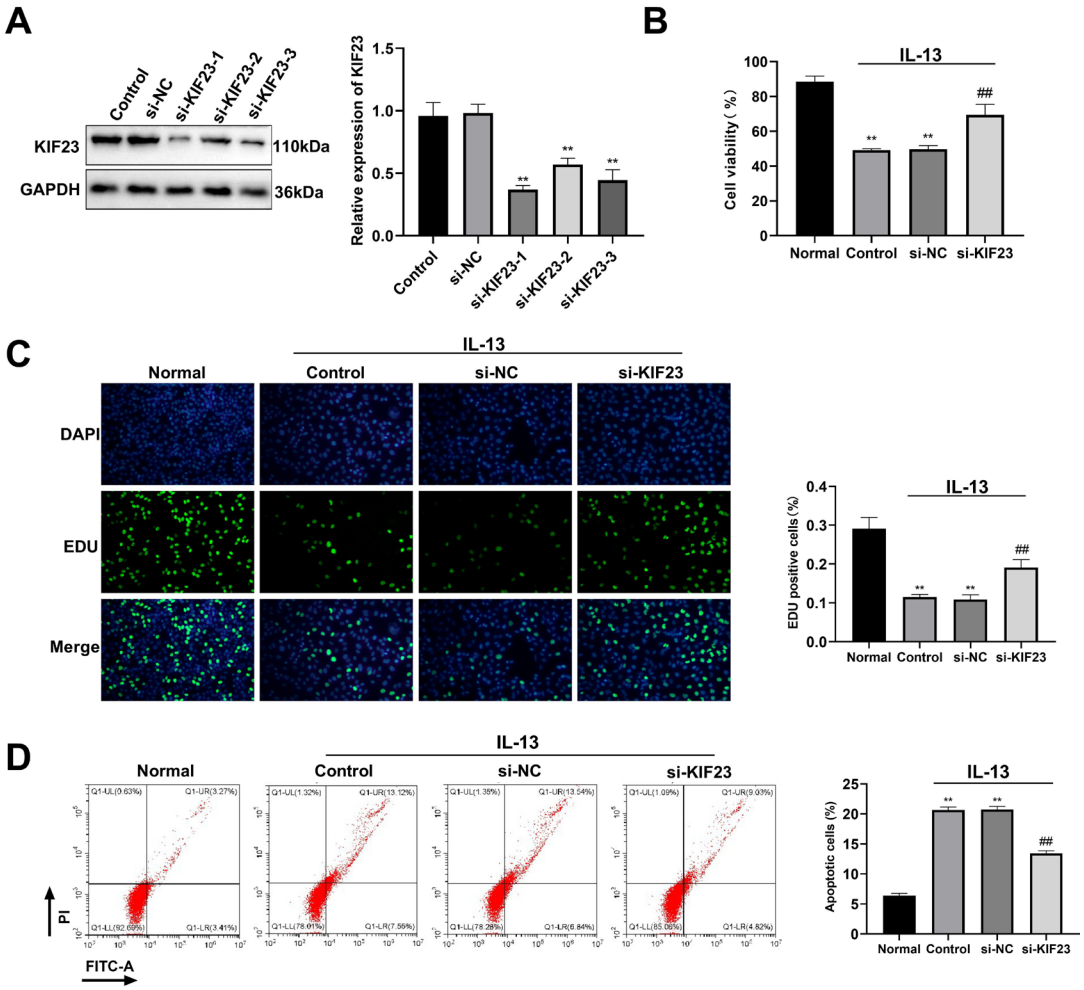

Figure 5 Knockdown of KIF23 increased cell proliferation and inhibited apoptosis of IL-13-induced BEAS-2B cells. (A) WB detection of si-KIF23 transfection efficiency. (B) CCK-8 detection of cell viability. (C) EdU detection of cell proliferation. (D) Flow cytometry detection of apoptosis. **P<0.01 vs normal group; ##p<0.01 vs si-NC group (n=3). CCK-8, cell counting kit-8; IL, interleukin; si-KIF23, cells were transfected with KIF23 siRNA-1/2/3; si-NC, cells were transfected with negative control siRNA; WB, western blot.

pairwise comparisons after ANOVA analysis. P<0.05 was considered statistically significant.

RESULTS

Establishment of asthma mouse model

Asthma mouse model was induced by OVA, and the experimental process was shown in figure 1A. The lung tissues of mice in both groups were taken for H&E staining (figure 1B), showing that the alveolar tissue of mice in the normal group had a clear structure and cellular hierarchy, the cells displayed a uniform and organised arrangement, and inflammatory cell infiltration was not seen. Compared with the normal group, there was a significant increase in the number of inflammatory cells, with slightly disordered cells, inconspicuous hierarchy, and condensed and solidified nucleus in the OVA-induced asthma group.

Immunohistochemistry was executed to detect the expression of caspase-3 (figure 1C). The results showed that there was a significant increase in caspase-3-positive colouring in the OVA group compared with the normal group. The expression of IgG and inflammatory factors in serum and BALF was detected by ELISA (n=6), showing that compared with the normal group, the levels of IgG and inflammatory factors (IL-1β, KC and TNF-α) in the serum and BALF were significantly increased in the OVA-induced asthma group (figure 1D–F).

Screening for DEGs and functional analysis

RNA-seq showed that there were 352 DEGs in the OVA-induced asthma group compared with the normal group, including 309 upregulated and 43 downregulated genes. The volcano plot and biocluster analysis of DEGs was drawn (figure 2A,B). Top 20 upregulated and downregulated DEGs were listed (online supplemental table 2 and figure 2A). The top 20 GO term entries with the most significant enrichment were selected for display, including cell cycle, cell

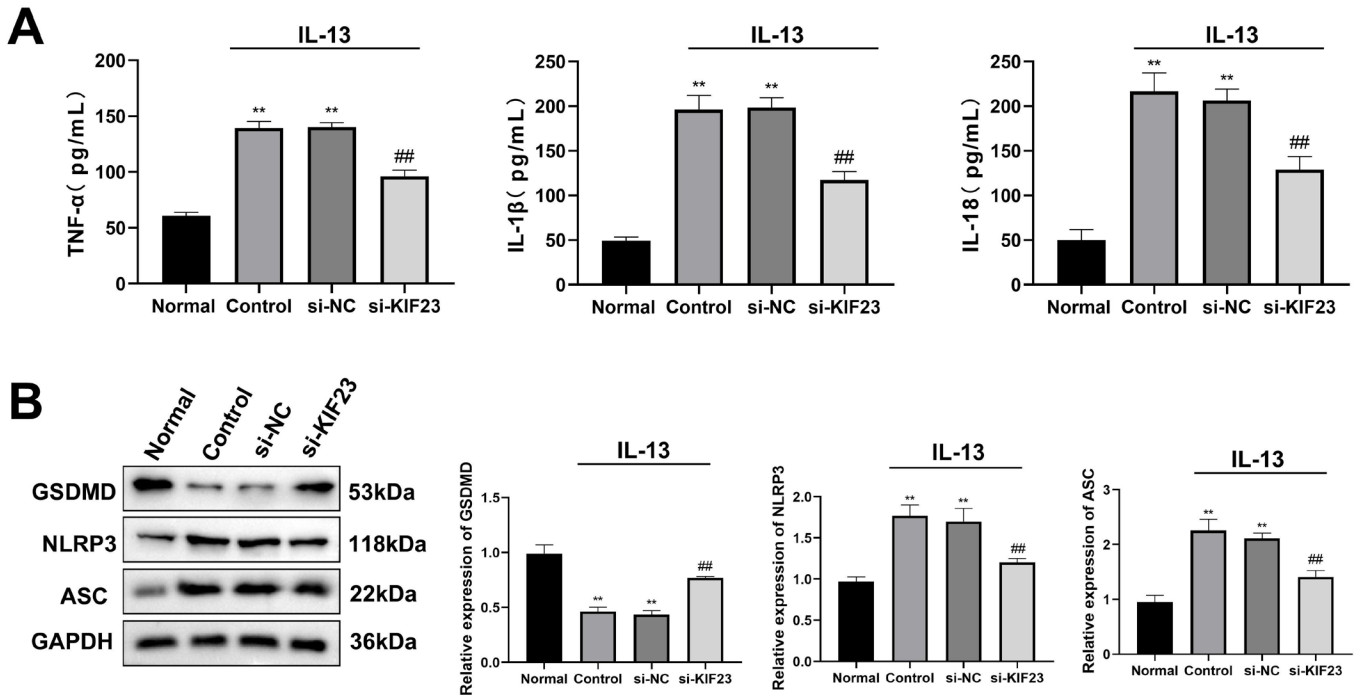

Figure 6 Knockdown of KIF23 inhibited inflammation and pyroptosis in IL-13-induced BEAS-2B cells. (A) ELISA detection of inflammatory factors (IL-18, IL-1β and TNF-α) expression. (B) WB detection of pyroptosis-related protein (GSDMD, NLRP3 and ASC) expression. **P<0.01 vs normal group; ##p<0.01 vs si-NC group (n=3). IL, interleukin; si-KIF23, cells were transfected with KIF23 siRNA-1/2/3; si-NC, cells were transfected with negative control siRNA; TNF, tumour necrosis factor; WB, western blot.

division, chromosome segregation, etc (figure 3A). In addition, the top 20 KEGG pathways were enriched, mainly including cell cycle, viral protein interaction with cytokine and cytokine receptor, etc (figure 3B).

Analysis of hub genes

The Venn diagram of DEGs and pyroptosis-related genes was drawn. The results showed that there were 11 common genes, including *Mpeg1*, *Cep55*, *Hsp90aa1*, *Trem1*, *Tlr8*, *Kif23*, *Pif1*, *Melk*, *Mki67*, *Il1rn* and *Trem2* (online supplemental figure 1A). Top seven genes with the highest score were displayed (online supplemental figure 1B). The levels of hub genes were detected by RT-qPCR (n=6). Compared with the normal group, the levels of *Melk*, *Kif23*, *Trem1*, *Mki67* and *Hsp90aa1* were significantly increased in the OVA-induced asthma group (p<0.01) (figure 4).

Knockdown of KIF23 promotes cell proliferation and inhibits apoptosis in IL-13-induced BEAS-2B cells

KIF23 was knocked down in BEAS-2B cells, and the silencing efficiency of KIF23 was detected by western blot (WB) (figure 5A). Compared with the si-NC group, the KIF23 protein was significantly reduced in the si-KIF23 group (including si-KIF23-1, si-KIF23-2 and si-KIF23-3) (p<0.01). The si-KIF23-1 was chosen for subsequent experiments, which had the best silencing efficiency.

Cell viability, proliferation and apoptosis of BEAS-2B cells in each group were detected by CCK-8, EdU assay and flow cytometry, respectively, demonstrating that compared with the normal group, the cell viability and proliferation were significantly decreased in the control and si-NC group, as well as the increased apoptosis rate (p<0.01, figure 5B–D). Compared with the si-NC group, si-KIF23 significantly promoted the cell viability and proliferation, while inhibited apoptosis rate of cells (p<0.01, figure 5B–D).

Knockdown of KIF23 inhibits inflammation and pyroptosis in IL-13-induced BEAS-2B cells

The expression levels of inflammatory factors in cells were detected by ELISA (n=3), showing that compared with the normal group, the levels of TNF-α, IL-1β and IL-18 were significantly elevated in the control and si-NC groups (p<0.01, figure 6A). Compared with the si-NC group, si-KIF23 significantly decreased the levels of TNF-α, IL-1β and IL-18 (p<0.01, figure 6A).

In addition, the levels of the key proteins of pyroptosis, GSDMD, NLRP3 and ASC, were detected by WB (n=3), illustrating that the levels of GSDMD were significantly reduced in the control and si-NC group compared with the normal group, as well as the increased NLRP3 and ASC expression (p<0.01, figure 6B). Compared with the si-NC group, GSDMD expression was significantly elevated, and NLRP3

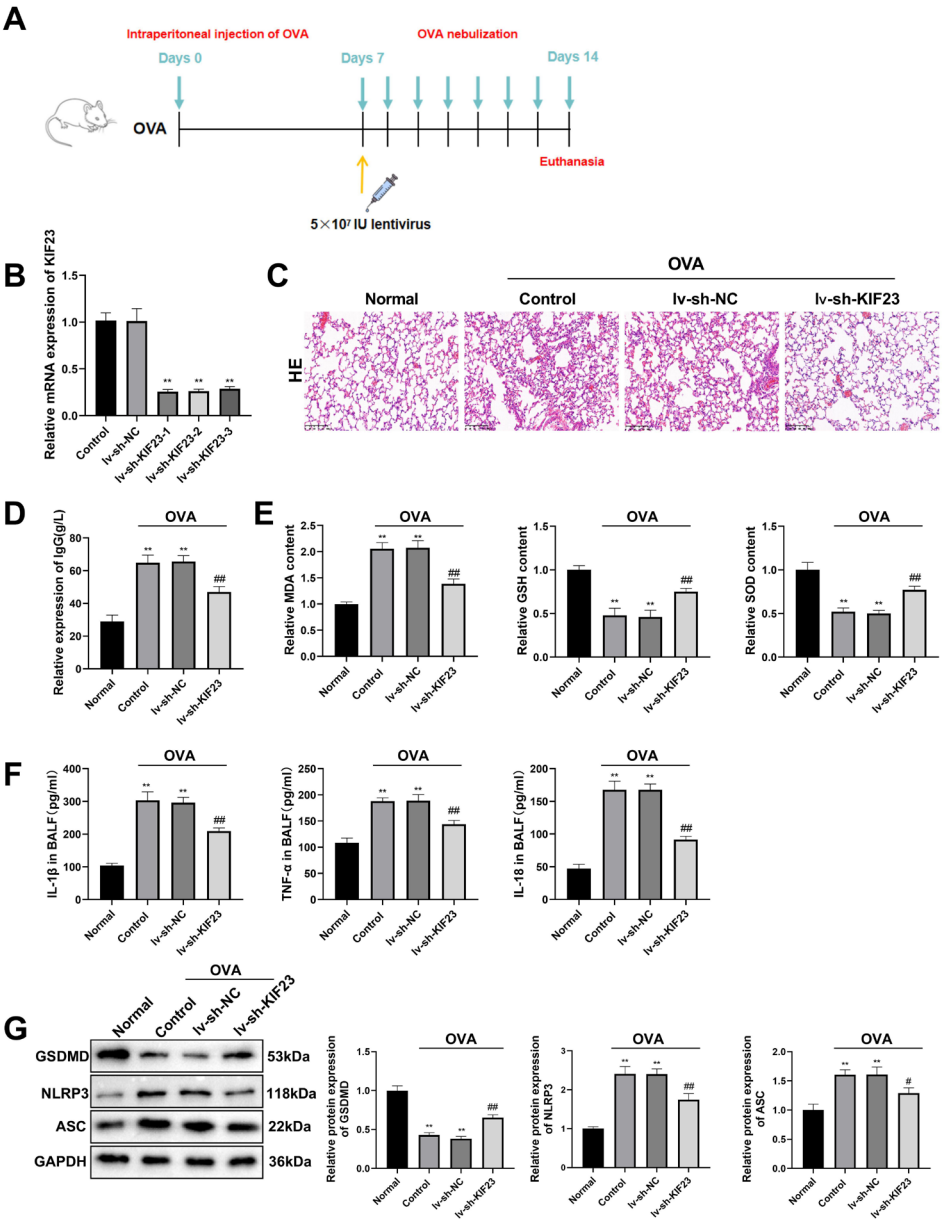

Figure 7 Knockdown of KIF23 suppressed inflammation, oxidative stress and pyroptosis to alleviate asthma in OVA-induced mice. (A) The schematic flow chart for mouse experiments. (B) RT-qPCR validation for KIF23 silencing efficiency. (C) H&E staining of lung tissues (magnification: 200×, scale bar: 100 µm). (D) ELISA detection of IgG level in mouse serum. (E) ELISA detection of oxidative stress markers (MDA, GSH and SOD) in mouse lung tissues. (F) ELISA detection of inflammatory factors (IL-18, IL-1β and TNF-α) in bronchoalveolar lavage fluid (BALF). (G) WB detection of pyroptosis-related protein (GSDMD, NLRP3 and ASC) expression. **P<0.01 vs normal group; ##p<0.01 vs lv-sh-NC group (n=6). IL, interleukin; lv-sh-KIF23, injected with lentivirus encoding *Kif23* shRNA; lv-sh-NC, injected with lentivirus encoding negative control shRNA; OVA, ovalbumin; RT-qPCR, real-time fluorescence quantitative PCR; TNF, tumour necrosis factor; WB, western blot.

and ASC were significantly decreased in the si-KIF23 group (p<0.01, figure 6B).

Knockdown of *Kif23* inhibits oxidative stress, inflammation and pyroptosis in OVA-induced mice

In vivo experiments were carried out to evaluate the effects of *Kif23* knockdown on the OVA-induced mice (n=6), and the schematic flow chart was displayed in figure 7A. RT-qPCR demonstrated that *Kif23* was successfully silenced in the lv-sh-KIF23 group, and lv-sh-KIF23-1 with the best silencing efficiency was chosen for following experiments (figure 7B). H&E staining was performed on the lung tissues of mice, demonstrating that compared with lv-sh-NC, knockdown of *Kif23* significantly reduced the number of inflammatory cells in the alveolar tissue of OVA-induced mice, with neatly arranged cells

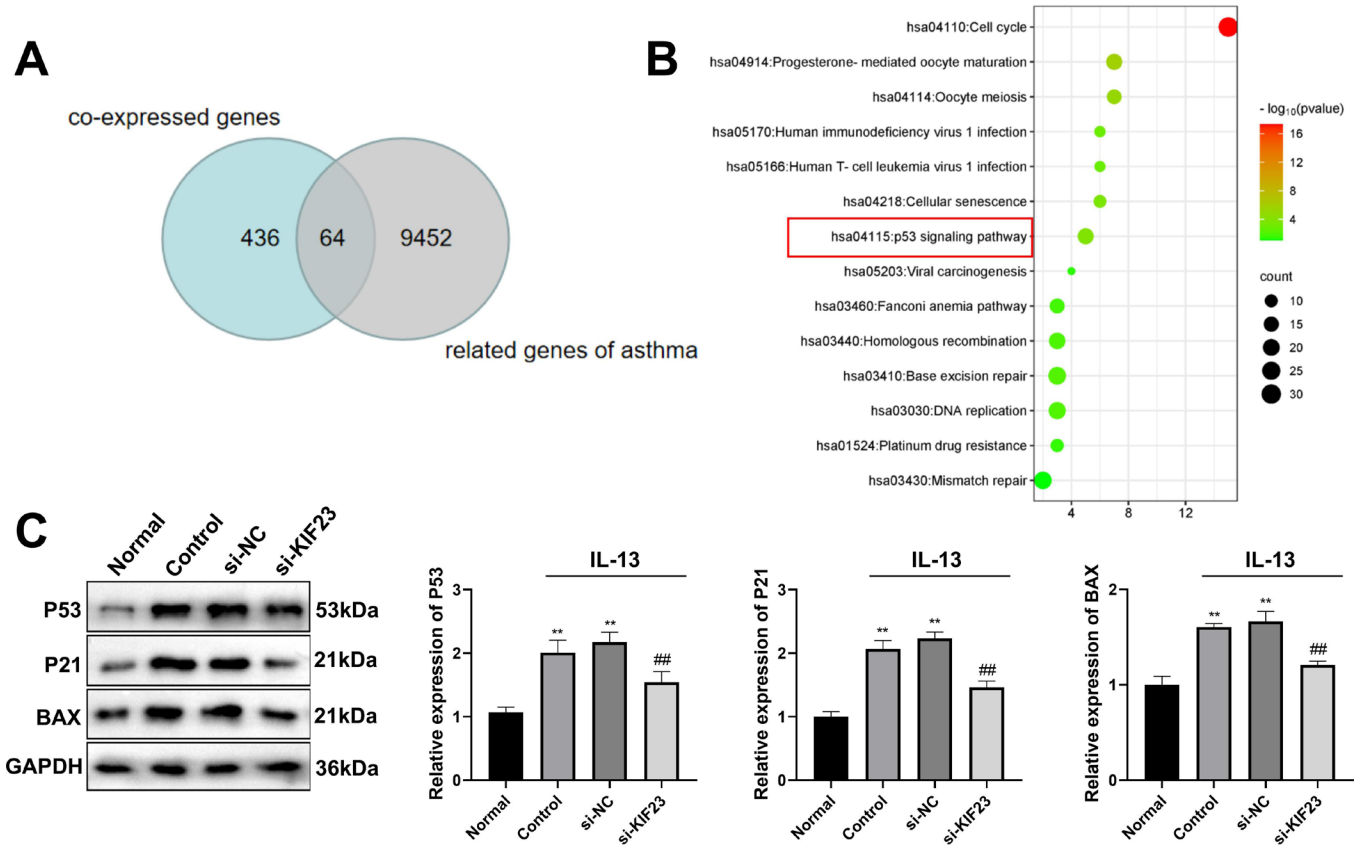

Figure 8 Knockdown of KIF23 inhibited p53 signalling pathway in IL-13-induced BEAS-2B cells. (A) Venn diagram. (B) Bubble plot of KEGG enrichment analysis. (C) WB detection of protein expression of p53, p21 and BAX. **P<0.01 vs normal group; ##p<0.01 vs si-NC group (n=3). IL, interleukin; KEGG, Kyoto Encyclopedia of Genes and Genomes; si-KIF23, cells were transfected with KIF23 siRNA-1/2/3; si-NC, cells were transfected with negative control siRNA; WB, western blot.

(figure 7C). In addition, IgG level, oxidative stress (MDA, GSH and SOD) and inflammatory factors (TNF-α, IL-1β and IL-18) in BALF were detected by ELISA, manifesting that knockdown of *Kif23* inhibited oxidative stress and inflammation in OVA-induced mice, while reduced the IgG level (p<0.01, figure 7D–F).

The expression levels of pyroptosis-related proteins in mouse lung tissues were detected by WB, demonstrating that compared with the normal group, there was a lower GSDMD level and higher NLRP3 and ASC levels in the control group, while knockdown of *Kif23* weakened the phenomenon in OVA-induced mice (p<0.01, figure 7G).

Knockdown of KIF23 inhibits p53 signalling pathway in IL-13-induced BEAS-2B cells

A total of 64 genes co-expressed with KIF23 in asthma were counted by Genecard and Coxpresdb databases (figure 8A). After KEGG enrichment analysis, bubble plot of KEGG analysis was drawn (figure 8B), in which p53 signalling pathway was significantly enriched. The expression levels of p53, p21 and BAX in each group were detected by WB (n=3), showing that compared with the normal group, the expression level of p53, p21 and BAX in the control and si-NC groups was significantly increased (p<0.01), and the expression levels of p53, p21 and BAX in the si-KIF23 group were significantly lower than those in the si-NC group (p<0.01, figure 8C).

DISCUSSION

Asthma is one of the most common chronic non-communicable diseases all over the world.[19 20] Its morbidity and mortality have improved significantly over the past 15 years.[20] However, the treatment is still insufficient. In this paper, the key gene *Kif23* was obtained by transcriptome analysis, and the regulatory effect of KIF23 was verified through the cell and mouse experiments. We found that knockdown of *Kif23* significantly promoted cell proliferation, inhibited apoptosis in the asthma cell model, while inhibited inflammation, oxidative stress and pyroptosis in vivo. Through bioinformatics analysis, the p53 signalling pathway and ferroptosis were enriched. It was proven that knockdown of KIF23 inhibited p53 signalling pathway and alleviated the progression of asthma by suppressing pyroptosis, providing a potential target for the therapy of asthma.

Through RNA-seq, hub genes, *Melk*, *Kif23*, *Trem1*, *Mki67* and *Hsp90aa1*, were identified by protein-protein interaction (PPI) network, indicating that they were closely in connection with the progression of asthma. Studies have reported that AURKA, MELK and TOP2A are key

genes in the pathogenesis of lung adenocarcinoma, and the high level of MELK is associated with the poor prognosis of lung adenocarcinoma.[21] Activation of TREM-1 can mediate mTOR-dependent mitochondrial fission and promote necroptosis of macrophages, thereby exacerbating acute lung injury.[22] Moreover, TREM-1 aggravates pulmonary fibrosis by aggravating senescence of mouse alveolar epithelial cells.[23] MKI67 is associated with cell proliferation and is a prognostic marker for multiple cancers, such as breast cancer.[24] Hachim *et al* have analysed hub genes associated with asthma and 10 hub genes including MKI67 are identified, finding that MKI67 is significantly upregulated in asthmatic bronchial epithelium and can be used as a reliable marker for asthma control.[25] HSP90AA1 is identified as one of the hub genes related to alveolar epithelial cell injury and may be involved in the progression of pulmonary acute respiratory distress syndrome.[26]

Currently, pyroptosis has become a research focus. Evidence has proved that pyroptosis can accelerate tumour proliferation, migration and invasion in cancer,[27] and is widely present in a variety of respiratory diseases. Schisandrin B restrains NLRP3 inflammasome activation and inhibits pyroptosis to alleviate airway inflammation and airway remodelling in asthma.[28] Targeting HDAC6 attenuates macrophage pyroptosis through the NF-κB/NLRP3 pathway and alleviates nicotine-induced atherosclerosis.[29] Wang *et al* have proved that IL-35 can inhibit inflammation and pyroptosis in TNF-α-induced bronchial epithelial cells, and it is found that the inhibition of pyroptosis can be achieved by suppressing the p38 MAPK pathway, thereby alleviating asthma.[30] Substance P, an 11 amino acid neuropeptide, activates the PI3K/AKT/NF-κB pathway, which triggers pyroptosis and leads to exacerbation of bronchial asthma.[31] In our study, knockdown of KIF23 significantly reduced the level of inflammatory factors, oxidative stress and pyroptosis in vivo and in vitro, while increased cell proliferation, indicating that knockdown of KIF23 inhibited inflammation and pyroptosis to alleviate asthma.

Tumour suppressor p53 is a transcription factor, which can inhibit cell proliferation or induce apoptosis.[32] Deficiency of the repressor element 1-silencing transcription factor contributes to p53-mediated cochlear cell apoptosis, leading to deafness.[33] Fortilin, an anti-p53 molecule, inhibits p53 to prevent cardiomyocyte apoptosis, protecting the heart from heart failure.[34] Furthermore, in bronchial epithelial cells, BMAL1/p53 mediates autophagy to exacerbate asthma induced by PM2.5.[35] In addition, the p53 pathway can also mediate pyroptosis to affect the development of several diseases. In clear renal cell carcinoma, silencing linc00023 significantly inhibits pyroptosis by regulating p53.[36] In non-small cell lung cancer, p53 inhibits tumour growth by promoting pyroptosis of cancer cells.[37] In previous study, KIF23 has been identified as a novel transcriptional target gene of p53,[38] which is similar to our results; knockdown of KIF23 significantly decreased the expression of p53, p21 and BAX, indicating that knockdown of KIF23 may inhibit the p53 signalling pathway. Like pyroptosis, apoptosis is also a programmed cell death mechanism.[39] The regulation of cell death is particularly important in the lungs. It is well-known that p53 can lead to apoptosis,[40] and apoptosis is proved to play a substantial role in asthma.[41] Studies have found that apoptosis of bronchial cells can promote airway damage, especially in patients with severe asthma.[42 43] Sesamin suppresses mitophagy and mitochondrial apoptosis to mitigate airway inflammation in asthma.[44] Similar to previous studies, in our study, knockdown of KIF23 significantly inhibited apoptosis and p53 signalling pathway in IL-13-induced BEAS-2B cells.

In conclusion, both in vivo and in vitro experiments have proved that knockdown of KIF23 significantly inhibits inflammation, apoptosis, oxidative stress and pyroptosis, suggesting that KIF23 knockdown has the potential to alleviate the progression of asthma, as well as inhibit the p53 signalling pathway. However, it is not clear whether KIF23 affects pyroptosis through p53 signalling pathway in asthma, which still needs to be further excavated in future studies.

Acknowledgements We would like to acknowledge the hard and dedicated work of all the staff.

Contributors XR was involved in the conception and design and drafted the paper. ZL and HZ were responsible for analysis and interpretation of the data. KL revised it critically for intellectual content. XR and CH approved the final version to be published. All authors are involved in the experimental process. XR agree to take responsibility and be accountable for the contents of the article.

Funding This work was supported by the Natural Science Foundation of Jiangxi Province (no. 20224BAB206009), Science and Technology Research Project of Jiangxi Provincial Department of Education (no. GJJ211528) and Ganzhou Guiding Science and Technology Plan Project (no. GZ2023ZSF114).

Competing interests None declared.

Patient and public involvement Patients and/or the public were not involved in the design, or conduct, or reporting, or dissemination plans of this research.

Patient consent for publication Not applicable.

Ethics approval In this study, all animal experiments confirmed to the Guide for the Care and Use of Laboratory Animals, and have been approved by the ethics committee of First Affiliated Hospital of Gannan Medical University (LLSC-2022090103).

Provenance and peer review Not commissioned; externally peer reviewed.

Data availability statement Data are available in a public, open access repository. The datasets used and/or analysed during the current study have been uploaded to NCBI SRA database (https://www.ncbi.nlm.nih.gov/sra/PRJNA1019821).

ORCID iD

Chaohua Hu http://orcid.org/0009-0002-9721-6459

REFERENCES

1 Mims JW. Asthma: definitions and pathophysiology. *Int Forum Allergy Rhinol* 2015;5:S2–6.
2 Sockrider M, Fussner L. What is asthma. *Am J Respir Crit Care Med* 2020;202:25–6.
3 Jones TL, Neville DM, Chauhan AJ. Diagnosis and treatment of severe asthma: a phenotype-based approach. *Clin Med (Lond)* 2018;18:s36–40.
4 Lemanske RF. Jr.: issues in understanding pediatric asthma: epidemiology and Genetics. *Journal of Allergy and Clinical Immunology* 2002;109:S521–4.
5 Miller RL, Grayson MH, Strothman K. Advances in asthma: new understandings of asthma's natural history, risk factors, underlying mechanisms, and clinical management. *J Allergy Clin Immunol* 2021;148:1430–41.
6 Fesquet D, De Bettignies G, Bellis M, *et al*. Binding of Kif23-Iso1/Cho1 to 14-3-3 is regulated by sequential Phosphorylations at two LATS kinase consensus sites. *PLoS One* 2015;10:e0117857.
7 Mishima M, Pavicic V, Grüneberg U, *et al*. Cell cycle regulation of central spindle assembly. *Nature* 2004;430:908–13.
8 Liu X, Gong H, Huang K. Oncogenic role of Kinesin proteins and targeting Kinesin therapy. *Cancer Sci* 2013;104:651–6.
9 Liu Y, Chen H, Dong P, *et al*. Kif23 activated WNT/B-Catenin signaling pathway through direct interaction with Amer1 in gastric cancer. *Aging* 2020;12:8372–96.
10 Jin C, Wang T, Zhang D, *et al*. Acetyltransferase Nat10 regulates the WNT/B-Catenin signaling pathway to promote colorectal cancer progression via Ac(4)C Acetylation of Kif23 mRNA. *J Exp Clin Cancer Res* 2022;41.
11 Gao C-T, Ren J, Yu J, *et al*. Kif23 enhances cell proliferation in Pancreatic Ductal adenocarcinoma and is a potent therapeutic target. *Ann Transl Med* 2020;8:1394.
12 Wu Z, Zhou G, Wang H, *et al*. Inhibition of Kif23 Alleviates IPAH by targeting Pyroptosis and proliferation of Pasmcs. *IJMS* 2022;23:4436.
13 Xia X, Wang X, Cheng Z, *et al*. The role of Pyroptosis in cancer: pro-cancer or Pro-"Host *Cell Death Dis* 2019;10:650.
14 Sun J, Li Y. Pyroptosis and respiratory diseases: A review of current knowledge. *Front Immunol* 2022;13:920464.
15 Cheng KT, Xiong S, Ye Z, *et al*. Caspase-11-mediated endothelial Pyroptosis underlies Endotoxemia-induced lung injury. *J Clin Invest* 2017;127:4124–35.
16 Song M, Wang J, Sun Y, *et al*. Inhibition of Gasdermin D-dependent Pyroptosis attenuates the progression of silica-induced pulmonary inflammation and fibrosis. *Acta Pharm Sin B* 2022;12:1213–24.
17 Zhuang J, Cui H, Zhuang L, *et al*. Bronchial epithelial Pyroptosis promotes airway inflammation in a murine model of toluene diisocyanate-induced asthma. *Biomedicine & Pharmacotherapy* 2020;125:109925.
18 Min Z, Zhou J, Mao R, *et al*. Pyrroloquinoline Quinone administration Alleviates allergic airway inflammation in mice by regulating the JAK-STAT signaling pathway. *Mediators Inflamm* 2022;2022:1267841.
19 Papi A, Brightling C, Pedersen SE. Reddel HK: asthma. *Lancet* 2018;391:783–800.
20 Porsbjerg C, Melén E, Lehtimäki L, *et al*. Asthma. *The Lancet* 2023;401:858–73.
21 Xu Y, Wang S, Xu B, *et al*. Top2A and MELK are the key genes identified by WGCNA for the pathogenesis of lung adenocarcinoma. *Oncol Lett* 2023;25:238.
22 Zhong W-J, Zhang J, Duan J-X, *et al*. TREM-1 triggers Necroptosis of Macrophages through mTOR-dependent mitochondrial fission during acute lung injury. *J Transl Med* 2023;21:179.
23 Xiong J-B, Duan J-X, Jiang N, *et al*. TREM-1 exacerbates Bleomycin-induced pulmonary fibrosis by aggravating alveolar epithelial cell Senescence in mice. *Int Immunopharmacol* 2022;113:109339.
24 Yerushalmi R, Woods R, Ravdin PM, *et al*. Ki67 in breast cancer: Prognostic and predictive potential. *Lancet Oncol* 2010;11:174–83.
25 Hachim MY, Elemam NM, Ramakrishnan RK, *et al*. Derangement of cell cycle markers in peripheral blood mononuclear cells of asthmatic patients as a reliable biomarker for asthma control. *Sci Rep* 2021;11:11873.
26 Chen H, Ding J, Xue H, *et al*. Snrna-Seq analysis reveals ten Hub genes associated with alveolar epithelial cell injury during pulmonary acute respiratory distress syndrome. *Heliyon* 2023;9:e17160.
27 Fang Y, Tian S, Pan Y, *et al*. Pyroptosis: A new frontier in cancer. *Biomedicine & Pharmacotherapy* 2020;121:109595.
28 Chen X, Xiao Z, Jiang Z, *et al*. Schisandrin B attenuates airway inflammation and airway remodeling in asthma by inhibiting Nlrp3 Inflammasome activation and reducing Pyroptosis. *Inflammation* 2021;44:2217–31.
29 Xu S, Chen H, Ni H, *et al*. Targeting Hdac6 attenuates nicotine-induced macrophage Pyroptosis via NF-KB/Nlrp3 pathway. *Atherosclerosis* 2021;317:1–9.
30 Wang Y, Yu Y, Yu W, *et al*. IL-35 inhibits cell Pyroptosis and attenuates cell injury in TNF-A-induced bronchial epithelial cells via P38 MAPK signaling pathway. *Bioengineered* 2022;13:1758–66.
31 Li M, Zhong X, Xu WT. Substance P promotes the progression of bronchial asthma through activating the Pi3K/AKT/NF-KB pathway mediated cellular inflammation and Pyroptotic cell death in bronchial epithelial cells. *Cell Cycle* 2022;21:2179–91.
32 Levine AJ. Levine AJ: P53, the cellular Gatekeeper for growth and division. *Cell* 1997;88:323–31.
33 Li H, Lu M, Zhang H, *et al*. Downregulation of REST in the Cochlea contributes to age-related hearing loss via the P53 apoptosis pathway. *Cell Death Dis* 2022;13.
34 Chunhacha P, Pinkaew D, Sinthujaroen P, *et al*. Fortilin inhibits P53, HALTS cardiomyocyte apoptosis, and protects the heart against heart failure. *Cell Death Discov* 2021;7:310.
35 Chen S-J, Huang Y, Yu F, *et al*. Bmal1/P53 mediating bronchial epithelial cell Autophagy contributes to Pm2.5-aggravated asthma. *Cell Commun Signal* 2023;21:39.
36 Zhu A, Cheng C, Lin S, *et al*. Silence of Linc00023 inhibits Pyroptosis and promotes cell proliferation via regulating P53. *Gene* 2023;882:S0378-1119(23)00469-9.
37 Zhang T, Li Y, Zhu R, *et al*. Transcription factor P53 suppresses tumor growth by prompting Pyroptosis in non-small-cell lung cancer. *Oxid Med Cell Longev* 2019;2019:8746895.
38 Fischer M, Grundke I, Sohr S, *et al*. P53 and cell cycle dependent transcription of Kinesin family member 23 (Kif23) is controlled via a CHR promoter element bound by DREAM and MMB complexes. *PLoS ONE* 2013;8:e63187.
39 Ketelut-Carneiro N, Fitzgerald KA. Apoptosis, Pyroptosis, and Necroptosis-Oh my! the many ways a cell can die. *J Mol Biol* 2022;434:167378.
40 Gottlieb TM, Oren M. Oren M: P53 and apoptosis. *Semin Cancer Biol* 1998;8:359–68.
41 Sauler M, Bazan IS, Lee PJ. Lee PJ: cell death in the lung: the apoptosis-Necroptosis axis. *Annu Rev Physiol* 2019;81:375–402.
42 Trautmann A, Schmid-Grendelmeier P, Krüger K, *et al*. Akdis CA: T cells and Eosinophils cooperate in the induction of bronchial epithelial cell apoptosis in asthma. *J Allergy Clin Immunol* 2002;109:329–37.
43 Cohen L, E X, Tarsi J, *et al*. Epithelial cell proliferation contributes to airway remodeling in severe asthma. *Am J Respir Crit Care Med* 2007;176:138–45.
44 Bai Q, Wang Z, Piao Y, *et al*. Sesamin Alleviates asthma airway inflammation by regulating Mitophagy and mitochondrial apoptosis. *J Agric Food Chem* 2022;70:4921–33.